AD-A079 118 NAVAL OCEAN SYSTEMS CENTER SAN DIEGO CA F/G 17/1
EFFECT OF UPDATE RANDOMIZATION ON REVGEN OUTPUT: MATCHED FILTER--ETC(U)
AUG 79 M E STEGMAN , J G MELVILLE
UNCLASSIFIED NOSC/TR-451 NL

1 OF 1
AD A079118

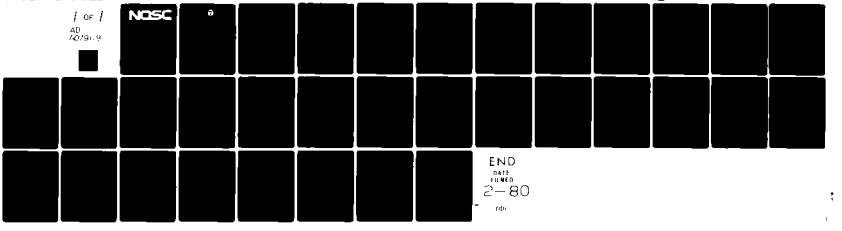

END
DATE FILMED
2-80
DDC

NOSC

NOSC TR 451

NOSC TR 451

Technical Report 451

EFFECT OF UPDATE RANDOMIZATION ON REVGEN OUTPUT: MATCHED FILTER PROCESSOR

ME Stegman and JG Melville

31 August 1979

Final Report: July 1978 — April 1979

Prepared for
Naval Sea Systems Command
(PMS 406)
Washington, DC 20362

Approved for public release; distribution unlimited

NAVAL OCEAN SYSTEMS CENTER
SAN DIEGO, CALIFORNIA 92152

NAVAL OCEAN SYSTEMS CENTER, SAN DIEGO, CA 92152

AN ACTIVITY OF THE NAVAL MATERIAL COMMAND

SL GUILLE, CAPT, USN
Commander

HL BLOOD
Technical Director

ADMINISTRATIVE INFORMATION

The work presented in this report was performed from July 1978 through April 1979 and was sponsored by the ALWT Project Office of the Naval Sea Systems Command.

Released by
RH Hearn, Head
Electronics Division

Under Authority of
DA Kunz, Head
Fleet Engineering Dept.

UNCLASSIFIED

SECURITY CLASSIFICATION OF THIS PAGE *(When Data Entered)*

REPORT DOCUMENTATION PAGE	READ INSTRUCTIONS BEFORE COMPLETING FORM
1. REPORT NUMBER: NOSC Technical Report 451 (NOSC TR-451)	2. GOVT ACCESSION NO. / 3. RECIPIENT'S CATALOG NUMBER
4. TITLE *(and Subtitle)*: EFFECT OF UPDATE RANDOMIZATION ON REVGEN OUTPUT: MATCHED FILTER PROCESSOR	5. TYPE OF REPORT & PERIOD COVERED: Final Report, July 1978–April 1979
	6. PERFORMING ORG. REPORT NUMBER
7. AUTHOR(s): ME Stegman and JG Melville	8. CONTRACT OR GRANT NUMBER(s)
9. PERFORMING ORGANIZATION NAME AND ADDRESS: Naval Ocean Systems Center, San Diego, California 92152	10. PROGRAM ELEMENT, PROJECT, TASK AREA & WORK UNIT NUMBERS: Project No. 63610N, SF 99-AS
11. CONTROLLING OFFICE NAME AND ADDRESS: Naval Sea Systems Command (PMS 406), Washington, D.C. 20362	12. REPORT DATE: 31 August 1979 / 13. NUMBER OF PAGES: 31
14. MONITORING AGENCY NAME & ADDRESS *(if different from Controlling Office)*	15. SECURITY CLASS. *(of this report)*: Unclassified / 15a. DECLASSIFICATION/DOWNGRADING SCHEDULE

16. DISTRIBUTION STATEMENT *(of this Report)*

Approved for public release; distribution unlimited

17. DISTRIBUTION STATEMENT *(of the abstract entered in Block 20, if different from Report)*

18. SUPPLEMENTARY NOTES

19. KEY WORDS *(Continue on reverse side if necessary and identify by block number)*

20. ABSTRACT *(Continue on reverse side if necessary and identify by block number)*

Rapid advancements in undersea weapon technology and signal processing have required improvements in accurate simulation of ocean reverberation. A NOSC effort in this area has included the implementation of REVGEN (a reverberation generation program developed by the Applied Physics Laboratory at the University of Washington). However, the requirement that this simulation operate in real time has required several simplifying modifications to the original REVGEN concept. This report examines the effect of various REVGEN algorithms on the output of a matched filter processor and, by analyzing the amplitude distribution of the range-Doppler

DD FORM 1 JAN 73 1473 EDITION OF 1 NOV 65 IS OBSOLETE
S/N 0102-LF-014-6601

UNCLASSIFIED

SECURITY CLASSIFICATION OF THIS PAGE *(When Data Entered)*

map, evaluates the resulting false alarm and detection statistics for the response of a two-dimensional variable threshold detector. Further, where changes in performance are significant, an alternate REVGEN algorithm is presented which is compatible with real-time operation on the NOSC Hybrid Simulator and, in some instances, actually reduces the computational requirements.

SUMMARY

OBJECTIVE

The objectives of this study were (1) to determine the effect of various REVGEN update algorithms on the output of a matched filter processor, and (2) to evaluate the resulting false alarm and detection statistics for the response of a two-dimensional variable threshold detector, which operates on the amplitude range-Doppler map.

RESULTS

REVGEN algorithms which restrict the number of updates and randomize in phase only, result in an artificial upper limit on large amplitude peaks in the range-Doppler map. Thus, they yield artificially low probabilities of false alarm. In addition, for a given signal-to-noise ratio, these lowered P_{FA} rates contribute to unreliably high probabilities of detection, due to incorrect placement of detection thresholds. Overall, it is seen that REVGEN algorithms, which generate relatively few fixed-amplitude updates, can have a significant effect on system performance.

RECOMMENDATION

Both theoretical and experimental evidence indicate that increasing the number of updates resolves the statistical disparity. More significantly, however, randomizing the update amplitudes according to a Rayleigh distribution produces proper single bin statistics independent of the update number. This decoupling of detection statistics from update number may, in some instances, permit reduction in REVGEN computational requirements by eliminating the need to process a large number of updates. Therefore, the randomization algorithm that is consistent with the physics of the medium and the REVGEN concept should provide for randomization both in phase and in amplitude.

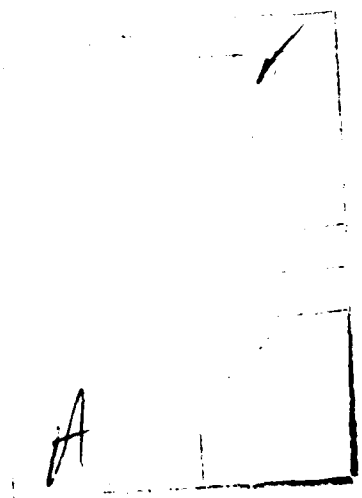

CONTENTS

1.0 INTRODUCTION

In the rapidly advancing areas of undersea weapon technology and signal processing, increased emphasis is being directed toward the development of techniques to produce accurate ocean reverberation signals. The use of computer simulation to model the ocean acoustical environment can reduce both the time and expense of actual at-sea studies, while providing the means for laboratory-based investigations essential to the development and testing of active sonar systems. Much effort has been focused on real-time implementation of REVGEN (Reverberation Generator) (ref. 1), a digital simulation of ocean reverberation.

At the base of the REVGEN concept is the assumption that reverberation may be represented by the linear process

$$Y = B\,X \tag{1}$$

where the column vector X is a sampled version of the transmit pulse, Y is a sampled version of the return echo, and the B matrix (a "large" set of complex numbers) contains the relevant information about the ocean environment and torpedo ocean interaction. The physical derivations of the original REVGEN concept are documented in references 1,3,4,5 but, as a brief outline, can be summarized in the following three-step process. First, a Doppler density matrix, $D_{J,K}$, is calculated from data defining the ocean environment and torpedo state (i.e., velocity, beam patterns, etc.) which in turn is used to form the B-matrix of equation (1). Finally, the B-matrix and samples of the transmit pulse can then be used to generate samples of a simulated reverberation return.

However, the requirement that this ocean reverberation algorithm operate in real time on the present NOSC, Univac 1110-based Hybrid Simulator has necessitated several alterations that simplify the original REVGEN concept. Although an accurate REVGEN computation would typically require calculating 256 rows of 256 Doppler density values every pulse length (τ_p), the current capacity of the simulator is to calculate one range slice of 256 Doppler values each τ_p. This disparity between the full number of range slices of $D_{J,K}$ and the fact that only one can be calculated per pulse length has led to certain "update" algorithms which serve to fill parts of the Doppler density matrix without resorting to lengthy calculation of the ocean algorithm. The ocean algorithm, used to construct the NOSC Doppler density matrix, partitions up the ocean into cells according to range and Doppler and then calculates the deterministic (mean) energy of the return from each cell according to the standard sonar equations (ref. 4). These values are then given complex random

---

[1] D.W. Princehouse, "REVGEN, A Real-Time Reverberation Generator -- Concept Development," Report No. 7511, Applied Physics Laboratory, University of Washington, September 1975.

[2] A.W. Rihaczek, "Principles of High Resolution Radar," McGraw-Hill, New York, 1969.

[3] D.W. Princehouse, "Reverberation Generator Ocean Algorithm, A Status Report," Report No. 7806, Applied Physics Laboratory, University of Washington, February 1978.

[4] B.A. Bologna and E.M. Rife, "Real-Time Ocean Model for Reverberation," Naval Ocean Systems Center, NOSC TN 383, March 1978.

[5] J.G. Melville and M.E. Stegman, "The Effect of Update Randomization on REVGEN Output: Broadband Energy Detector," Naval Ocean Systems Center, NOSC TR 292, August 1978.

phase and are loaded into the appropriate element of the matrix $D_{J,K}$. This departs from the true form of the matrix in two ways: first, the limited update algorithm severely reduces the number of non-zero matrix elements; second, these $D_{J,K}$ elements are assigned deterministic magnitudes (calculated from the sonar equations), when in reality they are stochastic in nature. This is due to the fact that, in practice, the ocean cells contain many randomly placed scatterers whose returns add coherently.

This report examines the statistical effect of these modifications (i.e., limited updates, fixed amplitudes) on detection processing of the simulated signals. (The statistical deviations addressed here, are similar to those presented in reference 5 for the response of a broadband energy detector.)

By analyzing the output range-Doppler map of a matched filter processor*, the remainder of this report examines the effect of simplifications of the REVGEN algorithm on corresponding probabilities of false alarm and detection. Further, where changes in performance are significant, an alternate algorithm is presented which is compatible with real time operation on the NOSC Hybrid Simulator and can be used to improve system performance.

2.0 THEORY

This section outlines the statistical nature of (1) the output obtained from matched filter processing of reverberation from point scatterers in an ideal ocean, (2) the corresponding analysis applied to REVGEN simulated returns, and (3) the resulting probabilities of false alarm and detection for the response of a two-dimensional variable threshold detector which operates on the amplitude range-Doppler map.

2.1 RANGE-DOPPLER MAP FOR POINT SCATTERER MODEL

The Generalized Point Scatterer Model, the physical model from which REVGEN was developed, assumes that reverberation is the sum of multiple reflections of the transmit pulse from point scatterers in the ocean medium. Each echo represents an individually amplitude-scaled, time-delayed, and Doppler shifted version of the transmitted waveform (ref. 1). This can be expressed mathematically (ref. 3) as:

$$Y(t) = \sum_{i=1}^{N_S} A_i \times \left[\gamma_i(t-\tau_i)\right] \; ; \qquad (2)$$

where,

- Y = reverberation signal (baseband complex)
- X = transmitted signal (baseband complex)
- A_i = complex amplitude of the i^{th} scatterer, including scatterer cross section, beam patterns, attenuation, propagation loss, and phase shift, if any, associated with reflection.

*Throughout this report, "matched filter" processing is used to refer to the operation of a "replicate correlator," which actually "matches" a replica of a transmit pulse to the return signal.

γ_i = Doppler shift of i^{th} scatterer (approximately $1 + 2V_i/C$)

V_i = speed of scatterer relative to transducer receiver

C = speed of sound, in water

τ_i = $(2\ R_i/C)$ = time delay of i^{th} scatterer

R_i = range of i^{th} scatterer, metres

N_s = total number of scatterers in ocean, a very large number.

For low Doppler targets and narrowband transmissions this can be rewritten in the approximate form

$$Y(t) = \sum_{i=1}^{N_s} A_i\, X(t-\tau_i)\, e^{j\omega_i\,(t-t_i)}\ ; \tag{3}$$

where, ω_i is the received-frequency-caused Doppler shifts of the individual scatterers.

Applying these results to the formula for $\chi(\tau,w)$, (ref. 2) the matched filter (replicate correlator) response in delay and Doppler gives:

$$\chi_{xy}(\tau,\omega) = \int_{-\infty}^{\infty} X(t)\, Y^*\,(t-\tau)\, e^{j\omega t} dt \tag{4}$$

$$= \int_{-\infty}^{\infty} X(t) \sum_{i}^{N_s} A_i \left[X(t-\tau)\, e^{j\omega_i (t-t_i)} \right]^* e^{j\omega t}\, dt$$

$$= \sum_{i} A_i^* \int_{-\infty}^{\infty} X(t)\, x^*\,(t-t_i-\tau)\, e^{j(\omega-\omega_i)t}\, e^{j\omega_i(\tau+t_i)}\, dt$$

$$\chi_{xy}(\tau,\omega) = \sum_{i} A_i^*\, \chi_{xx}(\tau + t_i, \omega - \omega_i)\, e^{j\omega_i(\tau+t_i)} \tag{5}$$

where χ_{xx} is the ambiguity function of the transmit pulse.

Thus, the output of the matched filter processor can be seen to equal the sum of multiple complex scatterer amplitudes which have been convolved with the ambiguity function of the transmit pulse, plus a phase term.

If the width of the main lobe of $\chi(\tau,\omega)$ is greater than a few wave lengths of the carrier frequency (which is almost always the case) and when there are a large number of scatterers within the "main lobe" then equation (5) represents the sum of a large number of randomly phased components. As such, $\chi(\tau,\omega)$ is a complex Gaussian random variable (by the law of large numbers) and $|\chi(\tau,\omega)|$ has a Rayleigh distribution. Ideally then, for the

point scatterer model of an ocean medium, the amplitudes of the output bins in the range-Doppler map will be distributed according to a Rayleigh distribution (ref. 6).

The foregoing has reviewed the statistical characteristics of the range-Doppler map produced from reverberation that would be received in an idealized (i.e., a homogeneous medium embedded with point scatterers), but real ocean environment. The following section discusses the effect of REVGEN simulation on corresponding matched filter output.

2.2 RANGE-DOPPLER MAP FOR REVGEN

The original REVGEN concept has been thoroughly documented in references 1,3 but is briefly outlined here to establish the basis of the relationship between the elements in the computer simulation and the resulting output of a matched filter processor.

Assuming that the ocean is a linear medium and that pulse compression or expansion can be approximated by frequency translation, the output REVGEN algorithm can be written in terms of the following matrix equation:

$$Y_J = \sum_L B_{J,L} X_L \tag{6}$$

where X_L represents a sampled vector of the transmit pulse and Y_J correspondingly represents the return signal. If X_L and Y_J are samples of the time series taken at intervals equal to the inverse of twice the respective bandwidths (ω_x,ω_y) of the transmit pulse and return echo, it can be shown that the B matrix contains all the information concerning the ocean medium that is available to that specific ping-echo process (ref. 1).

The B matrix is calculated[+] from the Doppler density matrix D, such that

$$B_{J,L} = \sum_{M=0}^{N-1} D_{J-L,M}\, e^{2\pi jML/N} \; ; \tag{7}$$

where, N is the number or transmit pulse samples in X,($L_{max} \leq N-1$), and J indexes the time of the echo return (ref. 1). The Doppler density matrix, D_{JM}, has elements that correspond to different range and Doppler returns in the echo. The rows of D_{JM} represent the spectral distribution of the scatterers at a particular range slice J. Throughout this report, the Doppler quantization or bin size is taken to be equal to $1/\tau_p$. This corresponds to the finest Doppler quantization available to a matched filter processor for a ping with that given length.

Given the Doppler density matrix, REVGEN then produces a complex time series (demodulated) which corresponds to the reverberation return. The elements of the Doppler density matrix, i.e.,

$$D_{J,K} = A_{J,K}\, e^{-j\phi_{J,K}} \tag{8}$$

---

[6]Rayleigh, "Scientific Paper," Vol. VI, Cambridge University Press, London, 1920.

[+]The sign in the exponent is somewhat arbitrary, the present convention is consistent with positive frequencies of the form $e^{i\omega t}$.

are computed (ref. 3) from the range- and Doppler-quantized, point scatterers of the Generalized Point Scatterer Model, equation (1), such that

$$D_{J,K} = A_{J,K}\, e^{-j\phi_{J,K}} \sum_{\substack{\text{certain} \\ i\text{'s}}} A_i\, e^{-j\phi_i} \quad ; \tag{9}$$

where, the sum is taken over those scatterers, i, which fall into the range cell J and Doppler cell K and where ϕ_i (and therefore the cumulative phase $\phi_{J,K}$) is a uniformly distributed random variable between zero and 2π. The effect of this quantization is discussed in reference 1 and is shown to be small.

Applying this result to equation (3) for the output of the matched filter processor, it is seen that for REVGEN returns the range-Doppler map will be determined by the sum f the amplitudes in the Doppler density matrix convolved with the ambiguity function of the transmit pulse. That is,

$$\chi(\tau,\omega) = \sum_{J,K} D_{J,K}\ \chi(\tau+\tau_j\ ,\ \omega-\omega_k)\, e^{j\omega_k(\tau+\tau_j)} \quad . \tag{10}$$

Using equation (9) and the fact that, independent of the distribution of any variable θ, $e^{j\phi+\theta}$ has uniform random phase if $e^{j\phi}$ is uniformly distributed in phase, it can be shown that equation (10) is equivalent to the randomly phased sum of the products of the magnitude of $D_{J,K}$ and the magnitude of the ambiguity function at the location specified by the J's and K's.

The following section compares this form of the equation with the original theory given in equation (5) and likewise compares the probability distributions for matched filter processing on the resulting time series.

2.3 EFFECT OF REVGEN MODIFICATIONS ON DETECTION STATISTICS

In the previous sections, two expressions were developed for the range-Doppler maps from an idealized point scattering model and for a range and Doppler quantized REVGEN calculation. While equations (5) and (10) are similar in form they can produce significantly differing returns. This section will explore some of these differences.

The primary difference between equations (5) and (10) is in the number of terms in the sum. The great reduction in number of terms, which comes with the REVGEN calculation, has its basis in equation (9) which shows how a large number of physical scatterers can be mapped into a single range-Doppler cell $D_{J,K}$. When this sum is performed, the $A_{J,K}$ values (for a given J and K) should be distributed according to a Rayleigh distribution, with a mean value which corresponds to the mean return from the portion of the ocean corresponding to the J,K range-Doppler interval. The mean returns can be calculated from the standard sonar equations and a knowledge of the torpedo beam patterns.

Up to this point, output of the point scattering model and the REVGEN calculation should be identical to within the processing constraints imposed by the input and output signal bandwidths.

The constraint that the entire reverberation calculation run in real time requires certain reductions to the original REVGEN algorithm. In particular, the number of times per pulse length that the ocean algorithm can be executed is very limited (currently only once per pulse length). Neither the point based method of equation (9) (which gives the proper randomness to $D_{J,K}$) nor even the deterministic calculation of $\overline{D_{J,K}}$ from the sonar equations can be calculated at the required rate (which can be up to hundreds of times per pulse length).

The current approximation make use of the fact that $\overline{D_{J,K}} \approx \overline{D_{J+\tau_p,K}}$ (i.e., the mean value of return averaged over many pings changes little over one ping length). Each ping length $D_{J,K}$ is calculated using the standard sonar equations for the range slice J and for all Doppler bins K. To fill in the Doppler Density matrix at update locations within one ping length, τ_p of J the following approximation is made $\overline{D_{J+\Delta J,K}} = \overline{D_{J,K}}$.

Randomness is introduced for each new update by multiplying terms D_{JK} by $e^{j\phi J+\Delta J,K}$ where $\phi J+\Delta J,K$ is selected randomly from a uniform distribution. The values $D_{J+\Delta J,K}$ are set equal to zero for $\Delta J = 1$ to $(N_{SAMP}/N)-1$, where N_{SAMP} is the number of range samples per ping length and N is the number of updates per pulse length.. The range slice $J+N_{SAMP}/N$ is then created, according to the relationship

$$D_{L,K} = D_{J,K}e^{j\phi\, L,K} \tag{11}$$

where

$$L = J+N_{SAMP}/N.$$

This procedure of re-randomizing (in phase only) the initial range slice and using it to "update" the Doppler-density matrix continues at regular intervals (N_{SAMP}/N) throughout the ping.

This undersampling of the Doppler-density further reduces the number of terms in equation (10) and can directly affect the statistics for the magnitude $|\chi(\tau,\omega)|$, of the output of a matched filter processor. When the $D_{J,K}$ are fixed according to a deterministic calculation of the standard sonar equations (ref. 4, based on the mean intensity of scatterers from within a certain volume) the sum $\chi(\tau,\omega)$ varies only according to phase angles and the shading applied by the ambiguity function. Therefore, equation (10) has an absolute limit for the possible values of $|\chi(\tau,\omega)|_{max} = \Sigma\, |\overline{D_{J,K}}^*|$.

Considering the probability distribution, it is consequently impossible to obtain arbitrarily large values of $|\chi(\tau,\omega)|$ beyond this implied maximum. (This is identical to the problem discussed in reference 5 for the envelope statistics of the complex time series generated by REVGEN.)

When the number of significant components in the sum (i.e., updates times the number of filled bins per update row) is large, this maximum value is large compared to the mean value and the distribution is more realistic in the tails; that is, as the number of updates increases, the distribution of the amplitudes in the range-Doppler map will approach a Rayleigh distribution. However, when the number of components is small (<20), significant differences can be noted in the shape of the tail of the distribution – the area crucial in determining false alarm rates. Since it is impossible to obtain values greater than the previously defined maximum, the probability distribution beyond this point drops sharply to zero. Applying this to the probability of false alarm, P_{FA}, which is determined by the area in the tail of the distribution beyond a set detection threshold, it is seen that as the placement of the detection threshold approaches the "drop-off" point, the values obtained for P_{FA} will be erroneously low.

However, there is an alternative to the time consuming process of increasing the number of updates in order to improve the statistics of REVGEN simulation. If the elements $D_{J,K}$ of the Doppler density matrix are randomized such that $A_{J,K}$ is Rayleigh distributed (with the mean of the distribution set by the deterministic sonar equation calculations), then the magnitudes $|\chi(\tau,\omega)|$ will have the proper statistical distribution independent of the number of elements used in the computation. In this case, equation (10) will be the sum of complex Gaussian random variables and is, therefore, itself a complex Gaussian random variable having the property that its magnitude $|\chi(\tau,\omega)|$ follows a Rayleigh distribution.

Therefore, a Rayleigh distribution of the magnitudes of the matched filter output can be achieved in either of two ways: (1) by using many updates, or (2) by randomizing the magnitudes of the Doppler density matrix elements according to a Rayleigh distribution. Thus, the REVGEN update algorithm used to generate the elements of the Doppler density matrix has a direct effect on the resulting output from a matched filter processor and can therefore alter the response of a two-dimensional variable threshold detector which operates on the amplitude range-Doppler map.

3.0 RESULTS

Based on the theories just presented, the results of this section provide graphic illustrations and experimental evidence of the effect various REVGEN update algorithms have on the probability statistics for the output from a matched filter processor. By analyzing the distribution of the amplitudes in the output bins (separated by $1/\tau_p$ in Doppler) of the range-Doppler map, the following figures provide a basis for comparing the various false alarm and detection statistics for the response of a two-dimensional variable threshold detector.

In addition to the predicted theoretical values, results are also demonstrated with actual REVGEN data. Computer simulation using a rectangular, CW transmit pulse, 20 channels and a three-second listening period generated 20 000 independent samples of the output range-Doppler map. To reduce the time and cost of computation it was determined that every eighth bin in each Doppler density row could be filled and still maintain independence between samples. Generally, it would be expected that some leakage would occur in adjacent bins. However, it can be shown that during simulations with 2, 4, and 8 updates per pulse length when the Doppler values are spaced with eight bin separation, all other non-zero elements of a row will not contribute the resulting matched filter output because the value of the ambiguity function will, in fact, be zero at these intervals. (See Appendix.)

3.1 DISTRIBUTION ANALYSIS

In the final theory section, emphasis was placed on the comparison of Rayleigh statistics for an idealized ocean model and the corresponding statistics for REVGEN return generated with relatively few, fixed amplitude, uniform phase distributed updates. It was shown that the output of a matched filter processor is significantly affected when REVGEN's updates are limited in number and fixed in amplitude. The comparison of figures 1 and 2 illustrates the effect of update randomization on the amplitude distribution of the matched filter output of actual REVGEN data which was generated with two updates per pulse

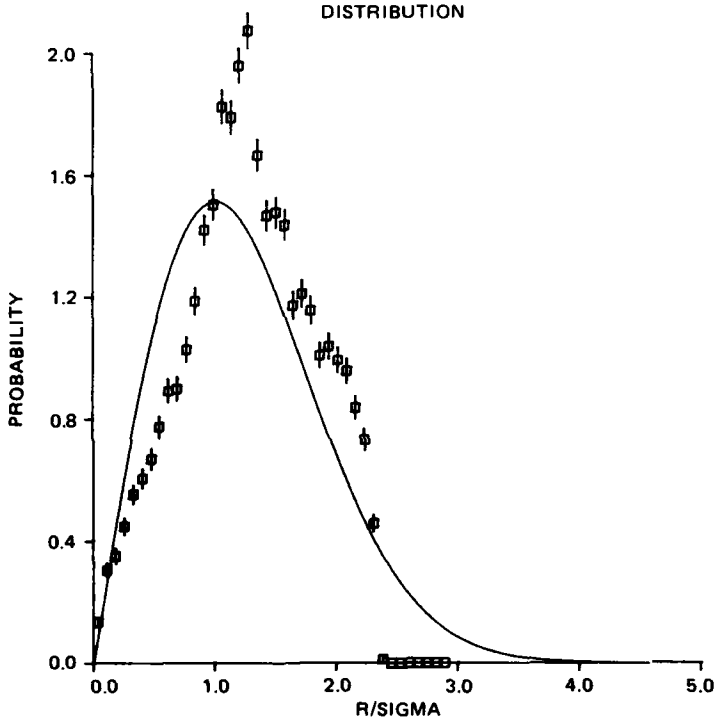

Figure 1. Theoretical probability distribution for Rayleigh model and experimental distribution (20 000 samples) for REVGEN with 2 updates per pulse length, fixed amplitudes, uniform random phase.

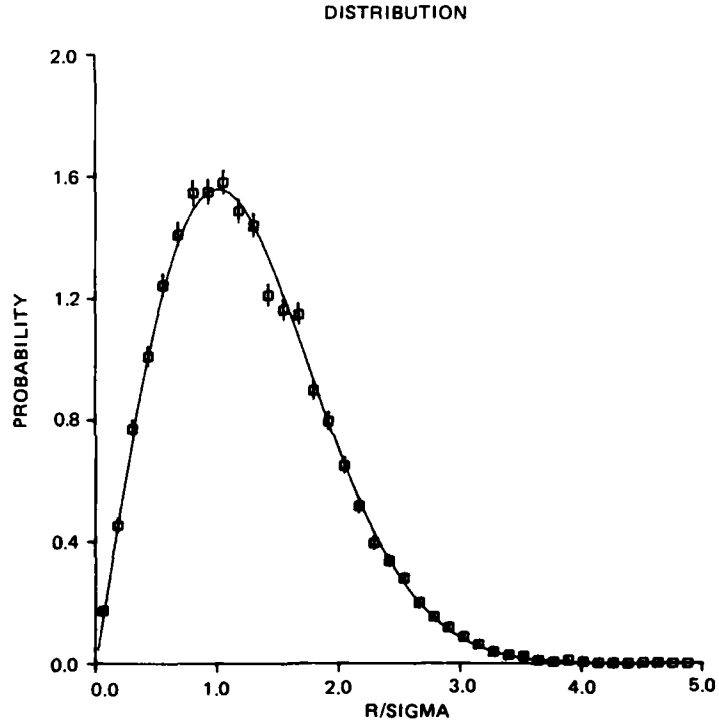

Figure 2. Same as figure 1 except the update algorithm uses 2 updates with Rayleigh randomized amplitudes, uniform random phase.

length. Figure 1 shows the distribution for updates of constant amplitude and uniform random phase. Figure 2 is the experimental result for a filtered REVGEN return when the two updates per pulse length were given Rayleigh randomized amplitudes. (In both figures, the solid line represents theoretical Rayleigh statistics with the same sample mean. Error bars represent one standard deviation.)

3.2 PROBABILITY OF FALSE ALARM

In processing simulated reverberation returns, a two-dimensional variable threshold detector operates on the amplitudes in the output bins of the range-Doppler map and responds with a "target" detection when this amplitude exceeds both a set detection threshold and a variable threshold based on the average amplitudes in surrounding bins. The altered amplitude statistics for D_{JK} shown in the previous section directly affect the probability of false alarm since it is precisely the probability of obtaining high amplitude range-Doppler peaks (i.e., the area in the upper tail of the distribution) which is critical in determining false alarm rates. The artificial upper limit caused by REVGEN algorithms which use relatively few updates, not-randomized in amplitude, results in artificially low values for P_{FA}.

In terms of equation (10), $|\chi_{xy}(\tau,\omega)|$ will approach a Rayleigh distribution even for updates whose magnitudes are constant if the number of $D_{J,K}$, which contribute significantly to the sum, is large. The exact weighting of each component is determined by ambiguity function $\chi_{xx}(\tau + \tau_J, \omega + \omega_K)$. For a square pulse, this function falls off rapidly in Doppler and relatively slowly in range (unless explicitly noted all analysis in this section refers to a square pulse envelope, the effect of pulse type is treated in the discussion section).

Figures 3 and 4 compare the effect on the false alarm rate (for a fixed threshold) of increasing the number of significant contributors to equation (10). This can be done in two ways, increasing the number of Doppler bins filled per range slice (figure 3) and by increasing the number of updates per pulse length (figure 4). In both cases, the curves were determined by first defining a set of amplitudes according of the ambiguity function and the positions of the filled bins in the proposed Doppler-density matrices. The problem of finding the distribution of the resultant of the vector sum of a finite set of randomly phased components (each having a specified length) was then solved as in reference 5. This technique was used to produce all the theoretical curves in the present report.

Figure 3 shows the probability of false alarm curves for various numbers of Doppler bins filled (centered on the maximum Doppler response of the ambiguity function) for eight updates per pulse length. As the number of filled bins increases, the probability of false alarm becomes more like the Rayleigh curve. However, since the ambiguity function ceases with increasing distance from the center bin, additional terms are of decreasing importance.

Figure 4 shows the probability of false alarm for various numbers of updates per pulse length when one bin is filled. The limits to the response, resulting from the small number components, is clearly seen. Note that even for eight updates per pulse length and a P_{FA} of 10^{-5}, the false alarm rate is more than an order of magnitude below the theoretical value.

For experimental support of the theories just presented, figures 5 through 7 present distributions of $|\chi_{xy}(\tau,\omega)|$ derived from 20 000 samples of the range-Doppler maps produced from actual REVGEN returns generated with 2, 4, and 8 updates per pulse

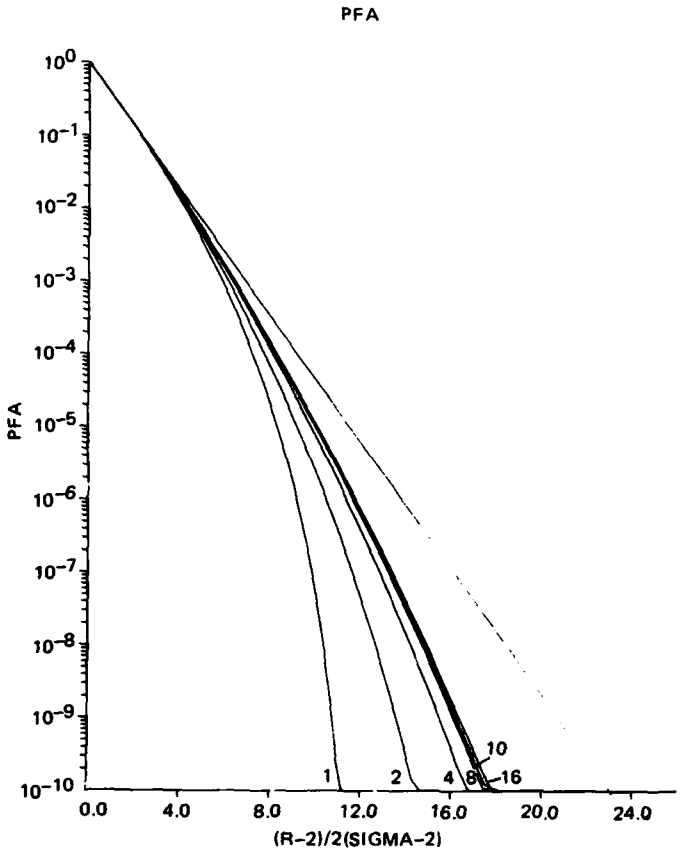

Figure 3. PFA versus threshold for 8 updates per pulse length, various bins filled, also PFA for Rayleigh distribution.

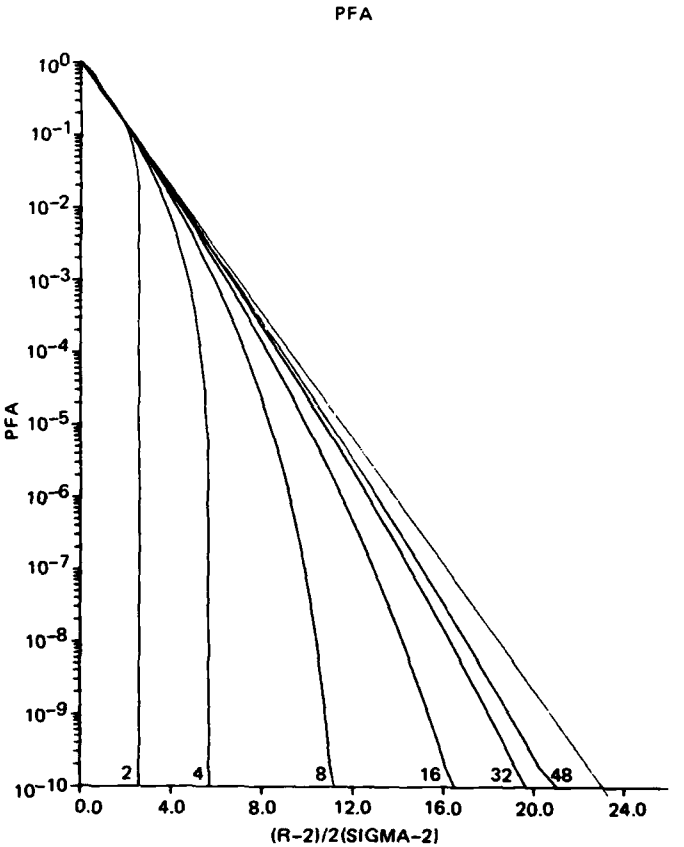

Figure 4. PFA versus threshold for various updates per pulse length (1 bin filled) and PFA for Rayleigh model.

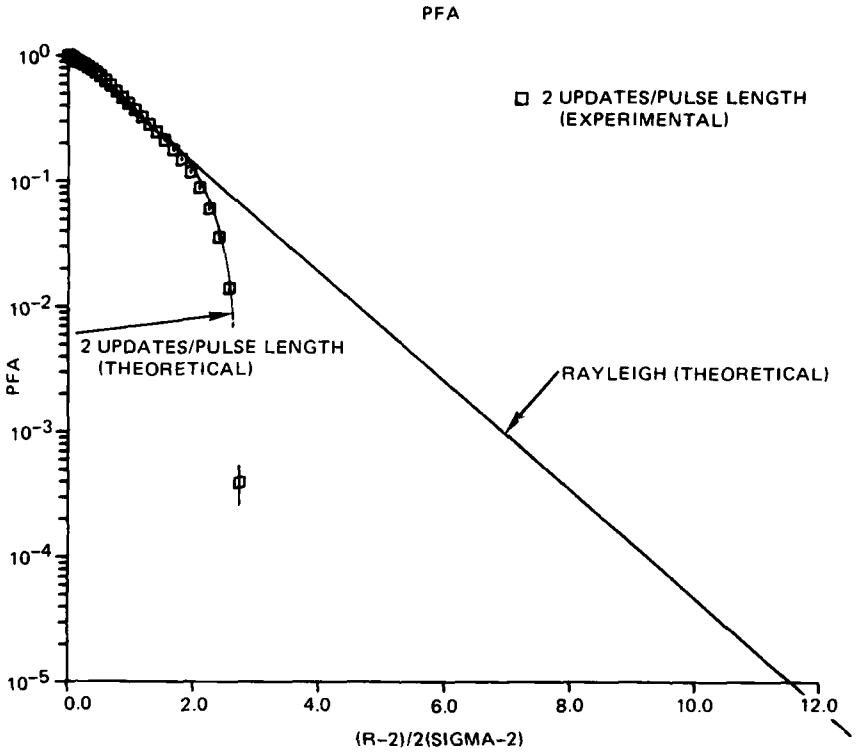

Figure 5. Experimental determination of PFA (20 000 points in sample) for a REVGEN signal with two updates per pulse length, constant amplitudes, rectangular transmit pulse, and uniform phase distribution. Error bars represent one sigma deviation. Solid lines are theoretical prediction for 2 updates (curve) and Rayleigh (straight).

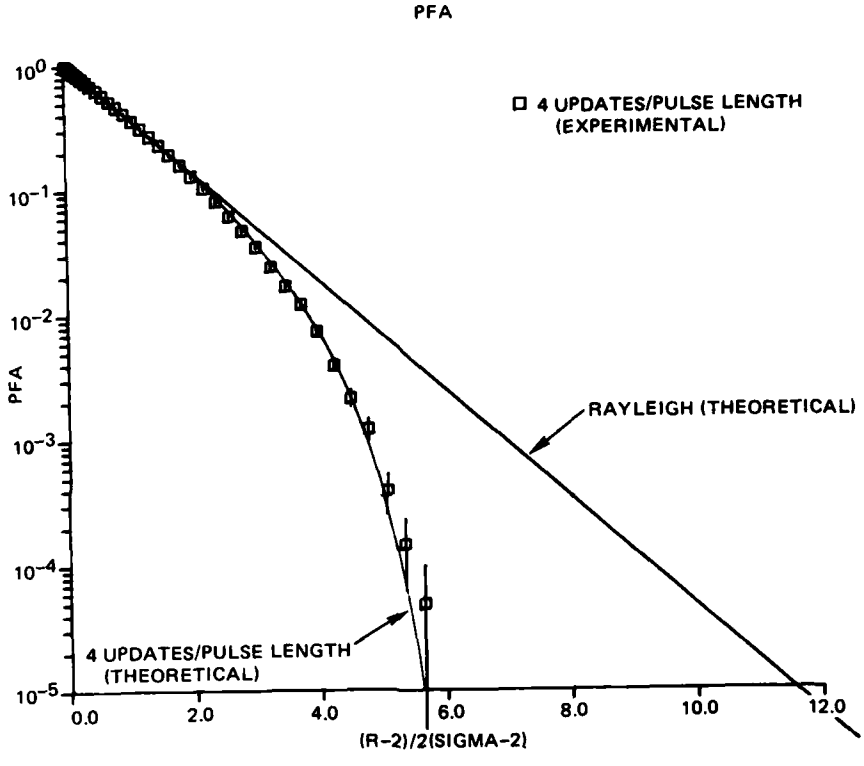

Figure 6. Same as figure 5 with 4 updates per pulse length, constant amplitudes.

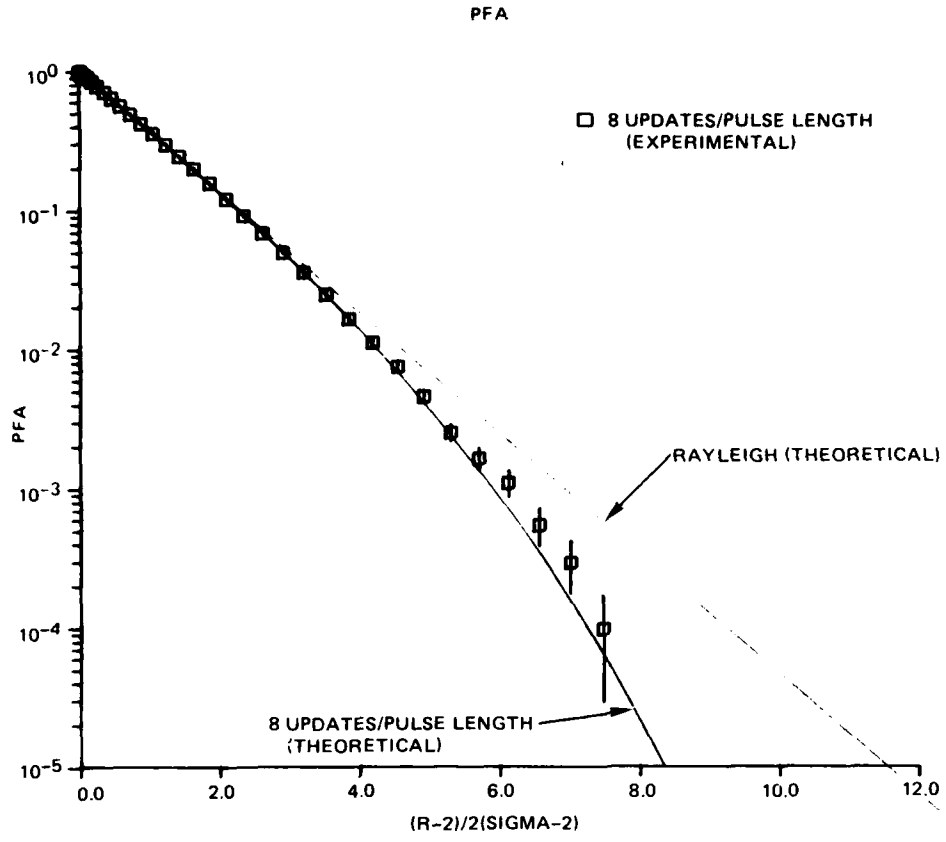

Figure 7. Same as figure 5 with 8 updates per pulse, constant amplitudes.

length (respectively), constant amplitude, a rectangular transmit pulse, uniform phase distribution and one filled Doppler bin. These computer simulations yielded results which are consistent with the theoretical values of figure 4 (1 bin filled) and also substantiate the predicted improvement caused by an increase in the update algorithm. (Error bars represent one standard deviation.)

For comparison, figure 8 presents a distribution derived from 20 000 samples of a REVGEN filtered return which were generated like those of figures 5 through 7, except that the amplitudes of the two updates per pulse length were randomized according to a Rayleigh distribution. Clearly, it is seen that while constant amplitudes require a large update algorithm to produce the proper statistics, Rayleigh randomized updates follow the Rayleigh statistical model independent of the number of updates used to generate the signal.

Table 1 provides further evidence that REVGEN algorithms, which randomize the elements of the Doppler density matrix in phase only, can cause artificial lowering of observed false alarm rates. Up to this point, it has been shown both theoretically and experimentally that the probability of false alarms is significantly effected by changes in the update algorithm. Table 1 summarizes actual test results of false detections which occurred

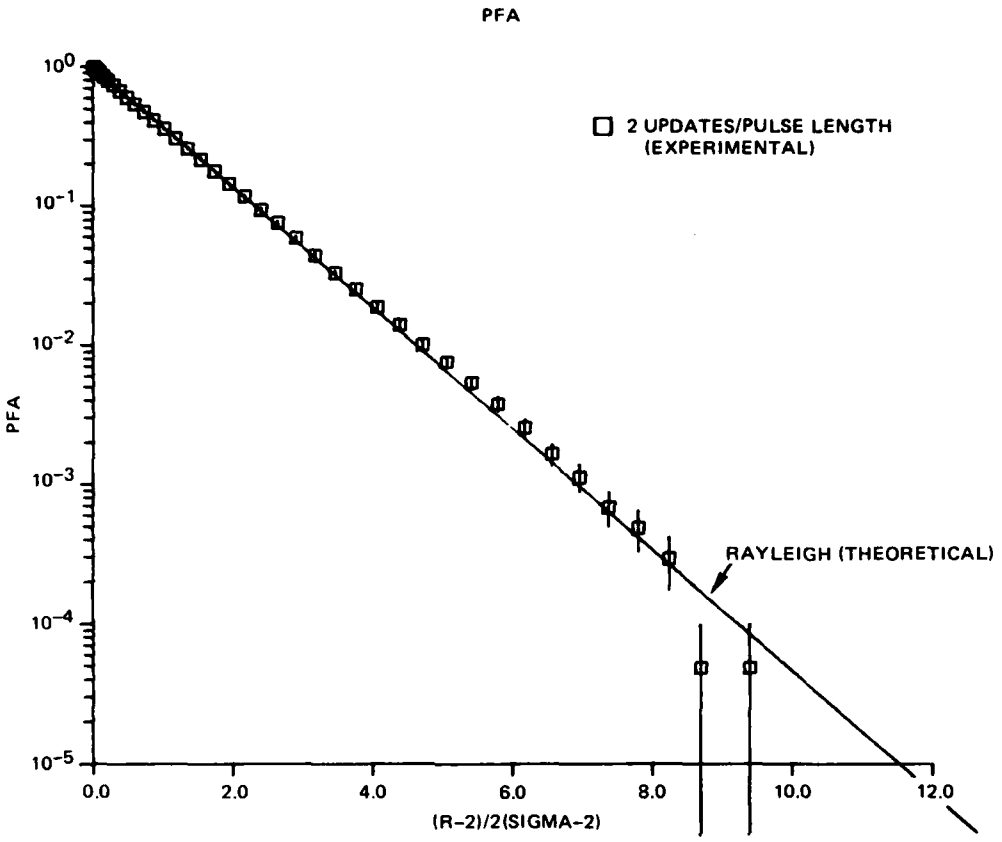

Figure 8. Same as figure 5 except the update algorithm uses 2 updates per pulse length having a Rayleigh distribution.

Table 1. Post detection editing false alarm rates.

REVGEN Update Algorithm	False Alarms
2 updates/pulse length Rayleigh randomized amplitudes, uniform phase	24 ± 5
8 updates/pulse length Rayleigh randomized amplitudes, uniform phase	26 ± 5
4 updates/pulse length fixed amplitudes, uniform phase	5 ± 3
8 updates/pulse length fixed amplitudes, uniform phase	9 ± 3

when a representative two-dimensional variable threshold detector was applied to the matched filter output (i.e., range-Doppler maps) of REVGEN signals generated with various update algorithms. In this case, all frequency bins were filled and the number of independent beams was increased until a significant number of false alarms had been detected for each of the update randomization schemes.

3.3 SNR POWER CURVES

The power curves shown in figures 9 through 11 are used to compare the relative accuracy of values obtained for the probability of detection (P_D) for differing numbers of updates per pulse length. Figures 9 through 11 set the detection threshold at a predetermined P_{FA} level and examine the resulting P_D values for various signal-to-noise ratios. Given the altered P_{FA} statistics just illustrated, it is clear that REVGEN update algorithms will likewise alter the SNR results, since these inaccurately low P_{FA} rates are those used to determine the placement of threshold. Thus, the focus of figures 9 through 11 indicates that at various SNR levels, the erroneously low P_{FA} values produce erroneously high P_D rates due to incorrect placement of the threshold.

The severity of this problem is somewhat dependent upon how the data is used. If the detection threshold is determined by taking a local average of values in the range-Doppler map and then setting the threshold based on the assumption of a true Rayleigh distribution, then the threshold will be close to the correct value and accurate values of P_D will be measured. However, in this case the P_{FA} values will be too low. If the data is used to experimentally set the detection threshold by measuring the false alarm rate, then the resulting P_D will be too high.

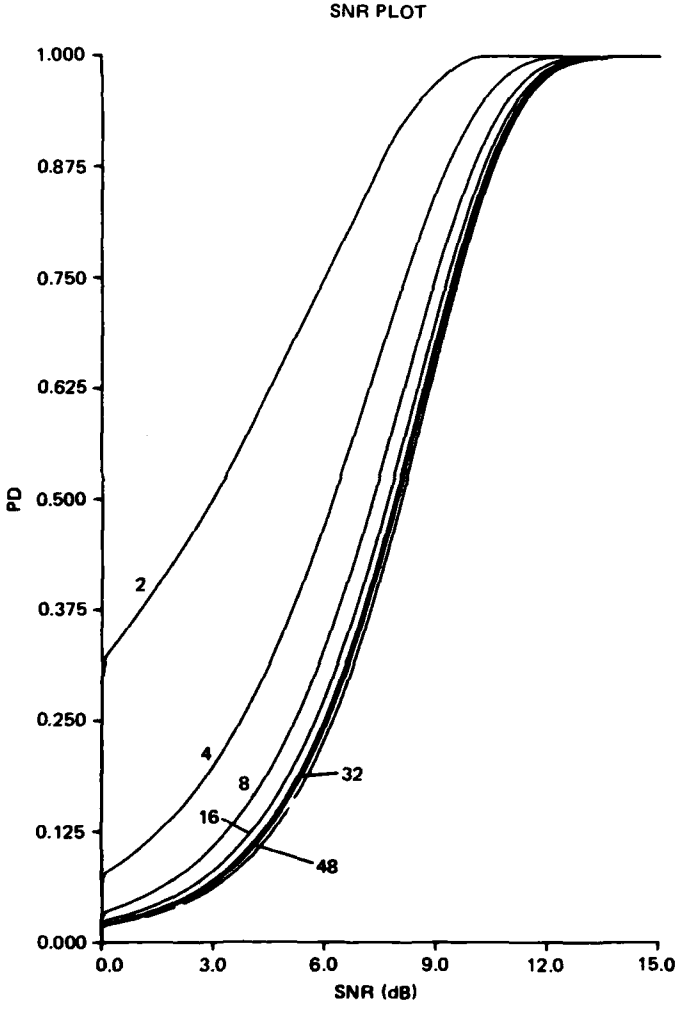

Figure 9. Probability of detection as a function of SNR (threshold set at PFA = 10^{-3}) for various update algorithms and for the Rayleigh case.

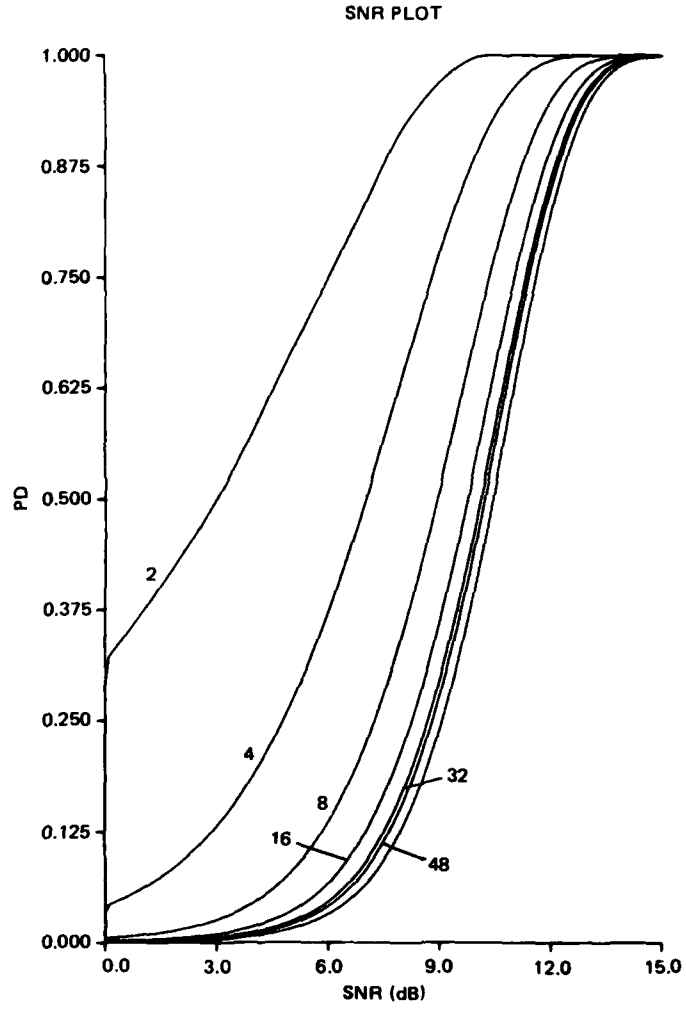

Figure 10. Same as figure 9 with PFA = 10^{-5}.

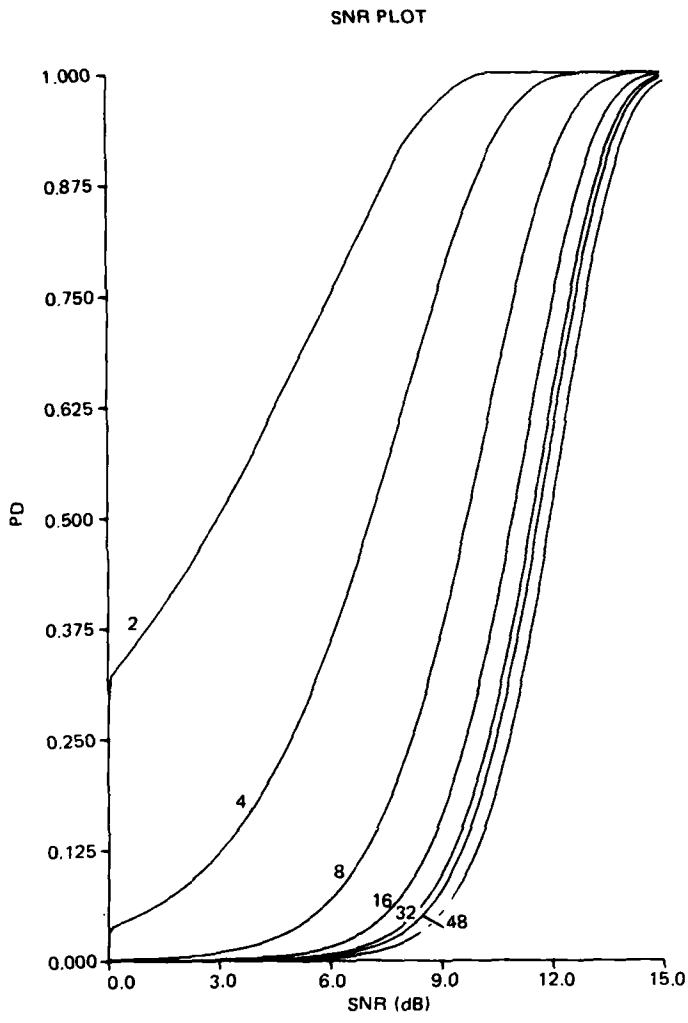

Figure 11. Same as figure 9 with PFA = 10^{-7}.

4.0 DISCUSSION

From the preceding sections, it is seen that the update algorithm used to generate REVGEN reverberation returns can directly affect the results of detection processing of the simulated signals. Both theoretical and experimental analysis of the output of a matched filter processor showed notably altered statistics for the probabilities of false alarm and detection when changes were made in the update algorithm.

Most significantly, it was shown that simulations which limit the number of updates per pulse length, while randomizing in phase only, yield artificially low P_{FA} rates and, therefore, affect proper placement of detection thresholds.

While increasing the number of updates seems to resolve the disparity, it was also shown that randomizing the magnitudes according to a Rayleigh distribution produces the proper distribution of values within a single range-Doppler bin, independent of the number of updates used in the simulation.

This decoupling of the detection statistics fro... the update algorithm may, in some instances, permit a reduction in the computational time needed for real-time implementation of REVGEN, by eliminating the need to process a large number of updates.

While, by using the proper randomization, the single bin values can be made to have the correct distribution with few updates per pulse length, there are other features of the range-Doppler map which remain sensitive to the number of updates used. These effects deal with bin-to-bin correlation in range and the relative mean value of the bins from one range to the next. A brief analysis is given to highlight these effects. For the numerical purposes of this analysis a rectangular transmit pulse envelope is assumed. This is noted where other pulse types would make a qualitative difference in the results. First, the bin-to-bin correlation is analyzed.

In mathematical terms the range-Doppler map results from the two-dimensional convolution of the ambiguity function of the transmit pulse with the Doppler density matrix, which for a point scattering model, is a finite set of delta functions distributed in range and Doppler (as in equation (5)). This ambiguity function has a value of one at its center and a non-zero value for a range extent of two pulse lengths.

As seen in equation (5), the sum $\chi(\tau,\omega)$ will include some of the same A_i's as the sum $\chi(\tau+\Delta\tau,\omega)$ (if $|\Delta\tau| < \tau_p$). Therefore, one would expect $\chi(\tau,\omega)$ to be correlated with $\chi(\tau+\Delta\tau,\omega)$ for $|\Delta\tau| < \tau_p$. In terms of a matched filter processor of the GCCD-type a bin-to-bin correlation in range is expected for range slices less than one pulse length apart.

It does not follow, that the correlation for a given overlap $(1-\Delta\tau/\tau_p)$ is independent of the number of updates. A few computer experiments were performed to demonstrate this.

For this case, of one Doppler bin filled with complex Gaussian random numbers (A_i), the value in the range-Doppler map χ_i at the given Doppler has the form

$$\chi_i = \sum_{j=-(N-1)}^{N-1} A^*_{i+j}\, R(J) \quad ; \tag{12}$$

where, N is the number of updates per pulse length, R(J) is the autocorrelation function of the transmit pulse and it is assumed that the χ_i is measured at the range corresponding to A_i. Equation (12) uses a single subscript for χ to denote the fact that only values at one particular Doppler are being calculated (the Doppler corresponding to the one filled bin).

For a rectangular transmit pulse R(J) = |N–J|/N, where J = –N to N and otherwise zero; therefore,

$$\chi_i = \sum_{j=-N-1}^{N-1} A^*_{i+j}\, \frac{|N-j|}{N} \quad . \tag{13}$$

Several series of χ_i were generated from random sequences of A_i's using equation (13) with successive values of the series corresponding to a change in the observation point of half the pulse length (i.e., $\Delta i = N/2$). This was done for N = 8, and N = 2.

The autocorrelation $R(\tau)$ function was then calculated for the function $|\chi_i|$ of the various series at the point $\tau = \tau_p/2$. The results of several series having the same N, but different random number sequences (A_i), were averaged and appear in table 2; also, included in this table are the corresponding correlations taken from the same REVGEN simulations used to produce the distributions reported earlier. Also, included for comparison are the correlation values for the REVGEN runs which randomized in phase only. The statistics of this problem are slightly different due to the randomization technique and so no predicted value is given.

A final entry in table 2 is the expected correlation when there is a very large number of updates. The calculation is similar to that described in chapter 4 of Ol'Shevskii (reference 7), except that the "signal envelope" in this context must refer to the ambiguity function rather than the envelope of the transmit pulse, as is the case when the correlation of the reverberation envelope function is sought. It can be shown that both problems have the same mathematical form, if the above substitution is made.

Table 2. Expected and observed correlation for matched filter outputs which are separated in range by half (square transmit pulse).

Number of Updates/Pulse	Magnitude Randomization	$R(\tau_p/2)$ from REVGEN	$R(\tau_p/2)$ from Eq. (12)	Theoretical (Ol'Shevskii)
2	Rayleigh	.435 + .007	.416 + .009	
8	Rayleigh	.495 + .05	.487 + .021	
2	Constant	.469 + .007		
8	Constant	.492 + .007		
Large	Rayleigh			.488

There are two general observations to be made from the data in table 2. The first, is that as the number of updates per pulse length is decreased the correlation is decreased between two bins in the range-Doppler map, separated in range by half a pulse length. The second, is that the theoretical value for large N is within the expected uncertainty of the correlation for eight updates per pulse length.

For shaped transmit pulses the ambiguity function falls off more rapidly in range than for a square pulse. This results in small weighting for those scatterers which would be common to two range-Doppler map values, separated by half a pulse length and consequently in a low bin-to-bin correlation for even large values of N.

The other general feature of the range-Doppler map, which changes with update number, is the expected mean value of $|\chi_i|$ at ranges between those range slices where scatterers were located in the Doppler density matrix. This effect can most easily be examined by again considering the case of a Doppler density matrix where only one bin is filled in Doppler and a square transmit pulse is used.

---

[7] V. V. Ol'Shevskii, "Characteristics of Sea Reverberation," Translated from Russian by Consultants Bureau, New York 1967.

If the scatterers have a complex Gaussian distribution with $\alpha = \alpha_j$ then the expected value of $|\chi(\tau)|$ is given by

$$\overline{|\chi(\tau)|} = \left[\sum_{j=N-1}^{N} (\sigma_j R(j+\tau))^2 \right]^{1/2} . \tag{14}$$

For the case N=2, $\sigma_j = 1$, and a rectangular transmit pulse with R(J) is a given in equation (13).

$$\overline{|\chi(0)|} = \left[\left(\frac{1}{2}\sigma\right)^2 + (1\sigma)^2 + \left(\frac{1}{2}\sigma\right)^2 \right]^{1/2}$$

$$= 1.22\sigma .$$

Here, $\overline{|\chi(0)|}$ indicates that $|\chi|$ is estimated at a point in the range-Doppler where one of the scatterers existed. In similar fashion, $|\chi(\tau_p/N)|$ is the estimated value of $|\chi|$ one update length away from the reference position (for a stationary process, with all propagation losses removed, one would expect $|\chi(0)| = |\chi(m\tau_p/N)|$ where m is an integer.)

In the above example the weightings of 1/2, 1, and 1/2 result from the form of the ambiguity function for a rectangular pulse. This is illustrated in figure 12.

If, however, $\overline{|\chi|}$ is to be estimated at a point half way in between scatterer locations, the shading of the ambiguity function (for N=2) is 1/4, 3/4, 3/4, and 1/4; therefore,

$$\overline{|\chi(\tau_p/4)|} = \left[\left(\frac{1}{4}\sigma\right)^2 + \left(\frac{3}{4}\sigma\right)^2 + \left(\frac{3}{4}\sigma\right)^2 + \left(\frac{1}{4}\sigma\right)^2 \right]^{1/2} = 1.12\sigma .$$

At $\tau_p/2$, the shading is the same as for $\chi(0)$ and therefore $\overline{|\chi(0)|} = \overline{|\chi(\tau_p/2)|}$.

As the number of updates per pulse length increases, the difference decreases between the maximum value (where the observation is at the same range slice as one of the scatters) and the minimum expected value (which occurs at a point half way between the scatters). A few sample curves showing this variation are shown in figure 13.

This figure shows curves for various pulse types and update numbers. For cosine and cosine squared weighted pulses, the following formulas were used for $R(\tau)$ (from reference 7):

for

$$S(t) = \cos(\pi t/\tau_p) , \quad |t| < \tau_p/2$$

$$R(\tau) = \frac{1}{\delta_{ef}} \frac{\tau_p - \tau}{2} \left[\cos(\pi\tau/\tau_p) + \frac{\tau_p}{2\pi} \sin(\pi|\tau|/\tau_p) \right] \tag{15}$$

$$\delta_{ef} = \tau_p/2$$

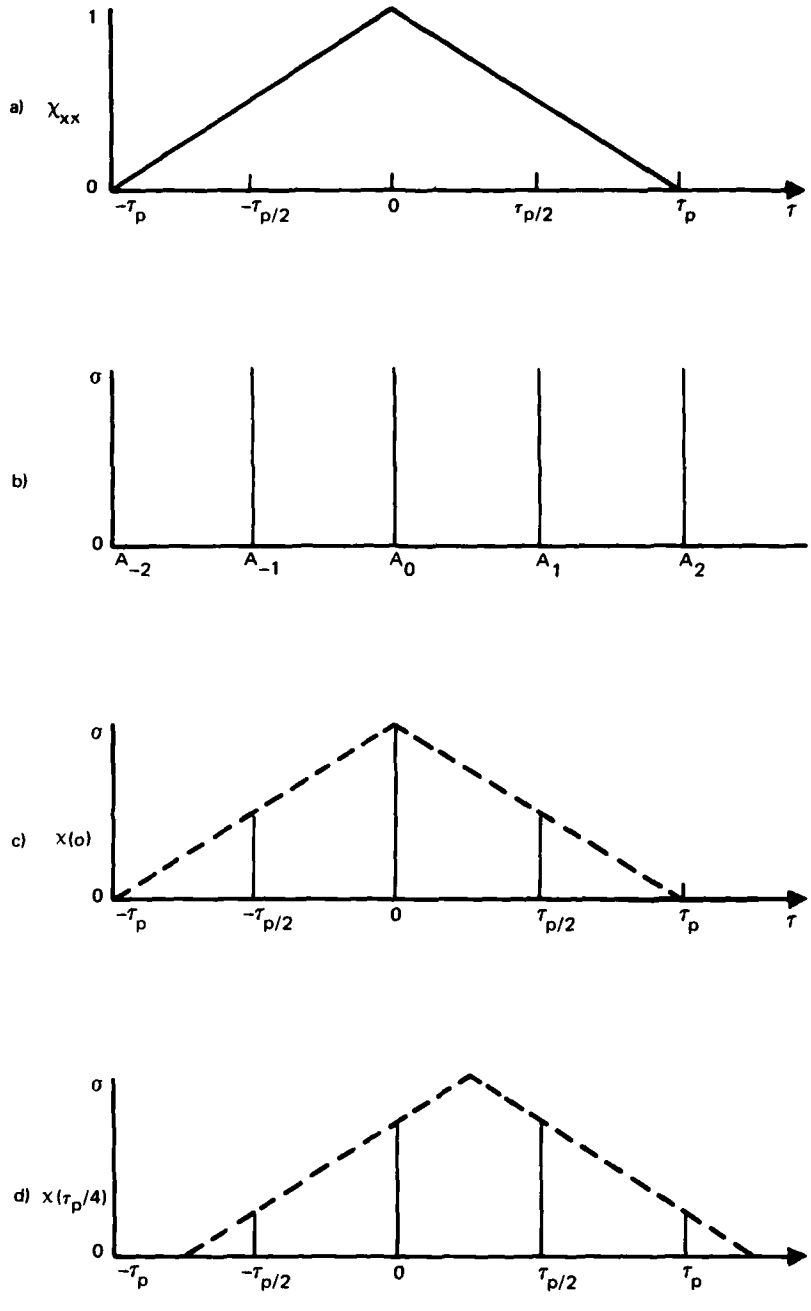

Figure 12. a) $\Delta\omega = 0$ slice of ambiguity function for square pulse of length τ_p b) one dimensional range doppler map c) representation of weighting function for $\chi(0)$ d) representation of weighting function for $\chi(\tau_{p/4})$.

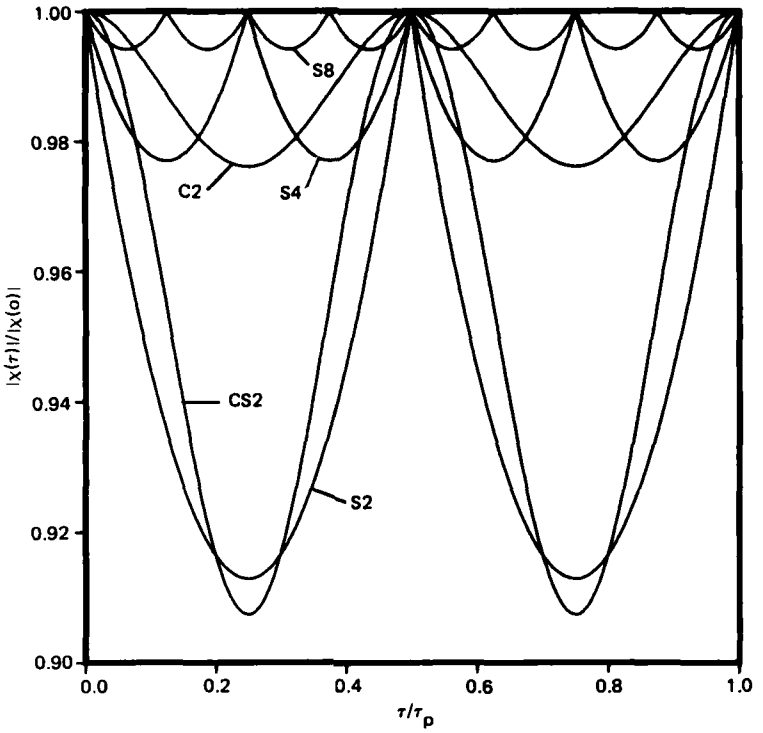

Figure 13. Curves of $|\chi(\tau)|/|\chi(0)|$ for various update rates and pulse types. S2 = square pulse, 2 updates, S4 = square pulse 4 updates, S8 = square pulse, 8 updates, C2 = cosine weighted pulse, 2 updates, CS2 = cosine squared weighted pulse, 2 updates.

and for

$$S(t) = \cos^2(\pi t/\tau_p), \quad |t| < \tau_p/2$$

$$R(\tau) = \frac{1}{\delta_{ef}}\left[\frac{\tau_p - \tau}{4} + \frac{\tau_p - \tau}{8}\cos\left(\frac{2\pi\tau}{\tau_p}\right)\right.$$

$$\left. + \frac{\tau_p}{4\pi}\sin(2\pi|\tau|/\tau_p) - \frac{\tau_p}{16\pi}\sin\left(\frac{2\pi|\tau|}{\tau_p}\right)\right] \qquad (16)$$

$$\delta_{ef} = \frac{3\tau_p}{8} \quad .$$

In general, the modulation in the amplitude of $|\chi|$ is slight. The worst case shown in the figure (two updates per pulse length with as $\cos^2$ transmit pulse) has a maximum deviation of χ^2 of 0.8 dB.

Table 3 contains numbers representing $|\chi(\tau)|/|\chi(0)|$ for several updated rates and pulse types where τ was chosen so that $|\chi(\tau)|$ is at a minimum. This again shows that, except for the case of one update per pulse length (shown separately in figure 14), the variation in $|\chi(\tau)|$ is small.

Table 3. Values of $|\chi(\tau_{min})|/|\chi(0)|$ for various updates per pulse length and pulse types. S = square pulse, c = cosine weighted pulse, cs = cosine squared pulse.

Updates	Pulse	τ_{min}	$\lvert\chi(\tau_{min})\rvert/\lvert\chi(0)\rvert$
1	S	$\tau_p/2$	0.707
1	C	$\tau_p/2$	0.450
1	CS	$\tau_p/2$	0.236
2	S	$\tau_p/4$	0.913
2	C	$\tau_p/4$	0.976
2	CS	$\tau_p/4$	0.907
4	S	$\tau/8$	0.977
4	C	$\tau/8$	0.999
4	CS	$\tau/8$	0.999
8	S	$\tau/8$	0.994
8	C	$\tau/8$	1.000
8	CS	$\tau/8$	1.000

The severity of this effect on a simulation will depend, in part, on how the range-Doppler map is sampled. If the difference in range between samples of the range-Doppler map (the FFT overlap is a matched filter type processor) is an integral multiple of the distance between updates in the Doppler density matrix, then the bin statistics should be stationary throughout a ping. Even in this case, small variations in the mean level of reverberation can occur from ping-to-ping, depending on where the initial sampling interval is placed with respect to the update scatterers. When the sampling frequency is not an integral divisor of the update rate the local mean reverberation level will vary periodically during the ping cycle.

Therefore, it is seen that one cannot arbitrarily reduce the update rate without affecting the nature of the REVGEN output. While the distribution of values in a single bin of the range-Doppler map is unaffected by update rate or pulse type, if a Rayleigh randomization is applied to the updates, the bin to bin correlation in range and the mean power per bin as a function of range are still affected. These last two factors then (upon applying the proper update randomization), become the critical issues in deciding upon the proper number of updates to use for simulation studies with matched filter type processors.

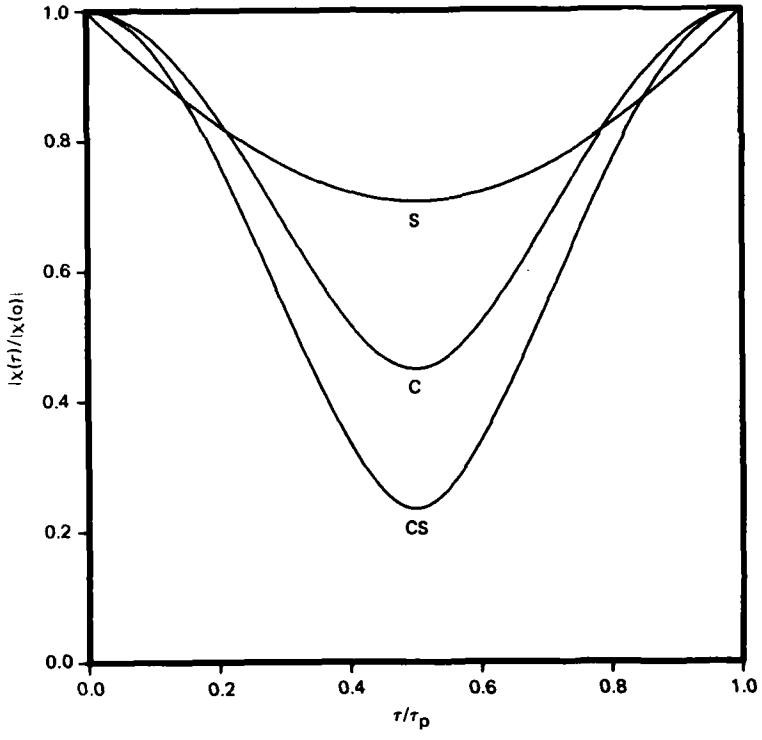

Figure 14. Curves of $|\chi(\tau)|/|\chi(0)|$ for one update per pulse length and various pulse types. S = square pulse, C = cosine weighted pulse, CS = cosine squared weighted pulse.

5.0 CONCLUSION

The conclusion to be drawn from the preceding paragraphs is that the REVGEN algorithm, which determines the number and randomization of the updates, has a direct effect on the output of a matched filter processor. This, in turn, can significantly affect the false alarm and detection statistics for target detectors which operate on the amplitude range-Doppler map.

Specifically, when the updates are limited (due to real-time restrictions) and randomized in phase only, the resulting P_{FA} statistics are artificially low; thus, forcing the placement of detection thresholds to be correspondingly inaccurate. Both theoretical and simulated evidence indicate that increasing the number of updates resolves the disparity. However, it is significant to note that Rayleigh randomized updates produce the proper single bin statistics, independent of the number of updates used in the simulation. Certain bin-to-bin characteristics are affected by reduction in update number, but these are small and the effects are well understood. The decoupling of the detection statistics from the update algorithm may, in some instances, permit reduction in REVGEN computational requirements by obviating the need to process a large number of updates per pulse length.

REFERENCES

1. D. W. Princehouse, "REVGEN, A Real-Time Reverberation Generator – Concept Development," Report No. 7511, Applied Physics Laboratory, University of Washington, September 1975.

2. A. W. Rihaczek, "Principles of High Resolution Radar," McGraw-Hill, New York, 1969.

3. D. W. Princehouse, "Reverberation Generator Ocean Algorithm, A Status Report," Report No. 7806, Applied Physics Laboratory, University of Washington, February 1978.

4. B. A. Bologna and E. M. Rife, "Real-Time Ocean Model for Reverberation," Naval Ocean Systems Center, NOSC TN 383, March 1978.

5. J. G. Melville and M. E. Stegman, "The Effect of Update Randomization on REVGEN Output: Broadband Energy Detector," Naval Ocean Systems Center, NOSC TR 292, August 1978.

6. Rayleigh, "Scientific Paper," Vol. VI, Cambridge University Press, London, 1920.

7. V. V. Ol'Shevskii, "Characteristics of Sea Reverberation," Translated from Russian by Consultants Bureau, New York 1967.

APPENDIX

To determine the form of the ambiguity function, consider the baseband equation (ref. 2)

$$\chi(\tau,\omega) = \int_{-\infty}^{\infty} x(t)\, x^*(t-\tau)\, e^{i\omega t}\, dt \;;$$

where x(t) is of the form $x(t) = e^{i\omega_o t}$ rect (t).

Substitution yields:

$$\chi(\tau,\omega) = \int_{-\infty}^{\infty} e^{i\omega_o t}\, \text{rect}\,(t)\, e^{-i\omega_o (t-\tau)}\, \text{rect}(t-\tau)\, e^{i\omega t}\, dt$$

$$= \int_{-\infty}^{\infty} e^{i\omega_o t}\, \text{rect}(t)\, e^{-i\omega_o t}\, e^{i\omega_o \tau}\, \text{rect}(t-\tau)\, e^{i\omega t}\, dt$$

$$= e^{i\omega_o \tau} \int_{-\infty}^{\infty} \text{rect}(t)\, \text{rect}(t-\tau)\, e^{i\omega t}\, dt \;;$$

which, integrated over the interval $T' = T - \tau$ gives

$$\chi(\tau,\omega) = \sum_{-T'/2}^{T'/2} e^{i\omega t}\, dt = \frac{1}{i\omega} e^{i\omega t} \Big|_{-T'/2}^{T'/2}$$

$$= \frac{1}{i\omega}\left(e^{i\omega T'/2} - e^{-i\omega T'/2}\right)$$

$$= \frac{1}{i\omega} 2i \sin\left[\omega T'/2\right]$$

$$= \frac{\sin\left[\omega T'/2\right]}{\omega/2}$$

$$= \frac{\sin\left[\omega(T-\tau)/2\right]}{\omega/2}$$

Writing ω in the form $\omega = (n/T)2\pi$, where ω_n is the frequency in the n^{th} Doppler bin, we can substitute

$$\chi(\tau,\omega) = \frac{\sin \omega(T-\tau)/2}{\omega/2} \quad ,$$

$$\chi(\tau,n) = \frac{\sin \frac{n}{T} 2\pi(T-\tau)/2}{\left(\frac{n}{T}2\pi\right)/2} = \frac{\sin n\pi\left(1-\frac{\tau}{T}\right)}{\frac{n\pi}{T}}$$

$$= \frac{(T-\tau)\sin n\pi\left(1-\frac{\tau}{T}\right)}{(T-\tau)\frac{n\pi}{T}}$$

$$= (T-\tau)\frac{\sin n\pi\left(1-\frac{\tau}{T}\right)}{n\pi\left(1-\frac{\tau}{T}\right)} \quad .$$

If normalized, so that $\chi(\tau,n) = 1$ and $\chi(0,0) = 1$ then

$$|\chi(\tau,n)| = \left(1-\frac{\tau}{T}\right)\frac{\sin(R)}{R} \qquad \text{where } R = n\pi\left(1-\frac{\tau}{T}\right),$$

which indicates that zeros of the ambiguity function will occur at bins where $n(1 - \tau/T)\pi$ is an integral multiple of π.

In the particular REVGEN case, where eight updates per pulse length are used,

$$\frac{\tau}{T} = \frac{m\Delta t}{T} = \frac{32m}{256} = \frac{m}{8}$$

and every eighth Doppler bin is filled (i.e., where bin n is a multiple of 8: $n = 8r$), substitution yields:

$$n\left(1-\frac{\tau}{T}\right)\pi = 8r\left(1-\frac{m}{8}\right)\pi = r(8-m)\pi \quad ,$$

an integral value of π whose $\sin [r(8-m)\pi] = 0$.

Therefore, in the special case of REVGEN where the Doppler bin separation is an integral multiple of the number of updates per pulse length, the bin centered value is the sole contributor in each row to the output of the matched filter processor.